

Contents lists available at ScienceDirect

Physics Letters B

www.elsevier.com/locate/physletb

Quasinormal modes in the background of charged Kaluza–Klein black hole with squashed horizons

Xi He^a, Bin Wang^{a,*}, Songbai Chen^{a,b}, Rong-Gen Cai^c, Chi-Yong Lin^d^a Department of Physics, Fudan University, 200433 Shanghai, China^b Institute of Physics and Department of Physics, Hunan Normal University, Changsha, 410081 Hunan, China^c Institute of Theoretical Physics, Chinese Academy of Sciences, PO Box 2735, 100080 Beijing, China^d Department of Physics, National Dong Hwa University, Shoufeng, 974 Hualien, China

ARTICLE INFO

Article history:

Received 18 February 2008

Received in revised form 1 June 2008

Accepted 17 June 2008

Available online 20 June 2008

Editor: T. Yanagida

PACS:

04.70.Dy

95.30.Sf

97.60.Lf

ABSTRACT

We study the scalar perturbation in the background of the charged Kaluza–Klein black holes with squashed horizons. We find that the position of infinite discontinuities of the heat capacities can be reflected in quasinormal spectrum. This shows the possible non-trivial relation between the thermodynamical and dynamical properties of black holes.

© 2008 Elsevier B.V. All rights reserved.

Quasinormal mode (QNM) of black holes has been an intriguing subject of discussions for the last three decades [1–3]. It is believed that QNM is a characteristic sound of black holes which could lead to the direct identification of the black hole existence through gravitational wave observations to be realized in the near future [1,2]. In addition to its potential astrophysical interest, theoretically QNM was believed as a tool to learn more about black hole and was even argued as a testing ground for fundamental physics. It was found that the QNMs of anti-de Sitter (AdS) black holes have direct interpretation in terms of the dual conformal field theory (CFT) [3–9]. This could serve as a support of the AdS/CFT correspondence. Attempts of using QNMs to investigate the dS/CFT correspondence have also been proposed [10]. Recently it was argued that QNMs might reflect the possible connection between the classical vibrations of a black hole spacetime and various quantum aspects by relating the real part of the QNM frequencies to the Barbero–Immirzi (BI) parameter, which was introduced by hand in order that loop quantum gravity reproduces correctly the black hole entropy [11,12]. But the direct connection has not been found in AdS black hole background [13].

It is of great interest to investigate whether QNM can reflect more physics of black holes. Recently some indications have been found that black hole phase transitions can show up in the QNM spectrum [14–16]. This is interesting since it might be the first phenomenon telling us the existence of the phase transition in black hole physics. In order to examine whether the QNM is an effective probe of phase transitions, we need to investigate more general black hole configurations with more general field perturbations. Jing et al. [17] computed the QNM of Reissner–Nordstrom (RN) black hole and claimed that they found the second order phase transition point predicted by Davies [18] where the heat capacity appears singular. However in [19], it was argued that the result in [17] might probably be a numerical coincidence and the conjectured correspondence between QNM and Davies's phase transition does not straightforwardly generalize to Kerr or Schwarzschild AdS metrics. Whereas calculations in [19] cannot rule out the relation between dynamical and thermodynamical properties of black holes but suggest that such a relation is non-trivial.

In the study of black hole phase transition, there have been a lot of debate on Davies' phase transition point. Around Davies' point, the black holes' event horizons do not lose their regularities and internal states of black holes do not change significantly. It was considered more reasonable that the phase transition of black hole occurs when a nonextremal black hole approaches its extremal limit, since all second moments of non-equilibrium fluctuations diverge there characterizing the second order phase transition [20]. Moreover extremal black holes are very different from nonextreme holes. Extremal holes just have superradiation but without Hawking radiation since its

* Corresponding author.

E-mail addresses: wangb@fudan.edu.cn (B. Wang), csb3752@163.com (S. Chen), cairg@itp.ac.cn (R.-G. Cai), lcyong@mail.ndhu.edu.tw (C.-Y. Lin).

Hawking temperature vanishes. The extremal black holes' geometric structures are also different from their nonextremal counterparts, since the singularity will be naked beyond the extremal limit. Davies' points for the divergence of the heat capacity were later proved in fact as turning points which are related to the changes of thermodynamical stability, especially in the canonical ensemble [21]. Whether the thermodynamical stability can be reflected from the dynamical stability such as the QNM spectra has been under heated discussions recently (for a review see [22]). For a black brane solution, it was argued that the thermodynamical stability is often related to dynamical stability [23]. But whether this correspondence is profound in all spacetimes is still not clear.

In this work we are going to study the QNM in the background of charged Kaluza–Klein (KK) black hole with squashed horizons [24] and investigate whether the QNM spectra can reflect the Davies' points of thermodynamical stability in this background. In [25], the thermodynamic properties of the KK black hole are discussed and compared to its undeformed five-dimensional RN black hole counterpart. The Davies' thermodynamical stability point was found where the heat capacity diverges when the horizon of the black hole crosses the critical value. We will examine the scalar perturbation in this background and see whether the thermodynamic stability can be reflected in the QNM spectrum.

The five-dimensional charged KK black hole with squashed horizons is described by [24]

$$ds^2 = -f(r)dt^2 + \frac{k^2(r)}{f(r)}dr^2 + \frac{r^2}{4}k(r)d\Omega^2 + \frac{r^2}{4}(d\psi + \cos\theta d\phi)^2, \tag{1}$$

where $d\Omega^2 = d\theta^2 + \sin^2\theta d\phi^2$ is the metric of the unit sphere and

$$f(r) = \frac{(r^2 - r_+^2)(r^2 - r_-^2)}{r^4}, \quad k(r) = \frac{(r_\infty^2 - r_+^2)(r_\infty^2 - r_-^2)}{(r_\infty^2 - r^2)^2}. \tag{2}$$

Here $0 < \theta < \pi$, $0 < \phi < 2\pi$ and $0 < \psi < 4\pi$ are Euler angles. The gauge potential is given by

$$A = \pm \frac{\sqrt{3}}{2} \left(\frac{r_+ r_-}{r^2} - \frac{r_+ r_-}{r_\infty^2} \right) dt. \tag{3}$$

As in the RN black hole, the coordinate singularities $r = r_+$ and $r = r_-$ correspond to the outer and inner horizons of the black hole, respectively. r_∞ is the spatial infinity. In the parameter space $0 < r_- \leq r_+ < r_\infty$, r is restricted within the range $0 < r < r_\infty$. The shape of black hole horizon is deformed by the parameter $k(r_+)$.

In the metric (1), the intrinsic singularity is just the one at $r = 0$. This can be seen by introducing a new radial coordinate ρ as

$$\rho = \rho_0 \frac{r^2}{r_\infty^2 - r^2}, \tag{4}$$

with

$$\rho_0^2 = \frac{k_0}{4} r_\infty^2, \quad k_0 = k(r = 0) = \frac{(r_\infty^2 - r_+^2)(r_\infty^2 - r_-^2)}{r_\infty^4}. \tag{5}$$

At the spatial infinity $r \rightarrow r_\infty$, $\rho \rightarrow \infty$. Thus in the new coordinate, ρ varies from 0 to ∞ when r changes from 0 to r_∞ . The metric (1) can be rewritten as

$$ds^2 = -F(\rho)d\tau^2 + \frac{K^2(\rho)}{F(\rho)}d\rho^2 + \rho^2 K^2(\rho)d\Omega^2 + \frac{r_\infty^2}{4K^2(\rho)}(d\psi + \cos\theta d\phi)^2, \tag{6}$$

with

$$F(\rho) = \left(1 - \frac{\rho_+}{\rho}\right) \left(1 - \frac{\rho_-}{\rho}\right), \quad K^2(\rho) = 1 + \frac{\rho_0}{\rho}. \tag{7}$$

Here we have defined the proper time $\tau = 2\rho_0 t / r_\infty$ for the observer at infinity. The mass and charge for this squashed KK black hole are defined by

$$M = \frac{3\pi r_\infty}{4G}(\rho_+ + \rho_-), \quad Q = \frac{\sqrt{3}\pi r_\infty}{G} \sqrt{\rho_+ \rho_-}, \tag{8}$$

where $\rho_\pm = \rho_0 r_\pm^2 / (r_\infty^2 - r_\pm^2)$ are the outer and inner horizons of the black hole in the new coordinate.

The Hawking temperature and entropy of the black hole can be expressed as [25]

$$T_H = \frac{\rho_+ - \rho_-}{4\pi \rho_+^2} \sqrt{\frac{\rho_+}{\rho_+ + \rho_0}} = \frac{r_+^2 - r_-^2}{2\pi r_+^3} \frac{r_\infty^2}{r_\infty^2 - r_-^2} \sqrt{\frac{r_\infty^2 - r_+^2}{r_\infty^2 - r_-^2}}, \tag{9}$$

$$S = 4\pi^2 (\rho_+)^{\frac{3}{2}} (\rho_0 + \rho_-)^{\frac{1}{2}} (\rho_0 + \rho_-) = \frac{\pi^2 r_+^3}{2} \frac{r_\infty^2 - r_-^2}{r_\infty^2 - r_+^2}. \tag{10}$$

Several limits of this charged squashed KK black hole were discussed in [24,25]. When $r_\infty \rightarrow \infty$, the squashing function k in (2) tends to be unity so that the metric (1) reduces to that of five-dimensional RN black hole. The entropy and the Hawking temperature also reduce to those of five-dimensional RN cases. When r_- goes to zero, we have the metric for the neutral black hole with squashed horizon. If we have $r_- = r_+$, we have deformed five-dimensional extremal RN black hole with one degenerate horizon whose Hawking temperature vanishes. For the case $r_+, r_- \rightarrow r_\infty$, with ρ_\pm finite, it is convenient to see from (6) that because $\rho_0 \rightarrow 0$, $K^2(\rho) \rightarrow 1$, the metric describes the four-dimensional RN black hole with a twisted S^1 bundle, where the size of the S^1 fiber takes the constant value $\sqrt{\rho_+ \rho_-} = r_\infty / 2$ [24]. Its temperature reduces to that of a four-dimensional black hole in this limit.

Table 1
Numerical data compared with H. Ishihara's work, with $\rho_0 = 0.5, \rho_+ = 1$

L	λ	WKB (6th order)	Frobrnius	Leaver
10	0	3.5194 - 0.15956i	3.510564 - 0.159674i	3.5105636 - 0.1596744i
10	1/2	3.5336 - 0.15821i	3.529225 - 0.158317i	3.5292246 - 0.1583174i
10	1	3.5898 - 0.15413i	3.585417 - 0.154231i	3.5854166 - 0.1542309i
10	3/2	3.6842 - 0.14729i	3.679778 - 0.147368i	3.6797783 - 0.1473680i
10	2	3.8178 - 0.13759i	3.813421 - 0.137647i	3.8134213 - 0.1376469i
10	5/2	3.9924 - 0.12493i	3.988012 - 0.124944i	3.9880116 - 0.1249440i
10	3	4.2103 - 0.10912i	4.205922 - 0.109076i	4.2059218 - 0.1090755i
10	7/2	4.4747 - 0.08988i	4.470523 - 0.089745i	4.4705233 - 0.0897455i

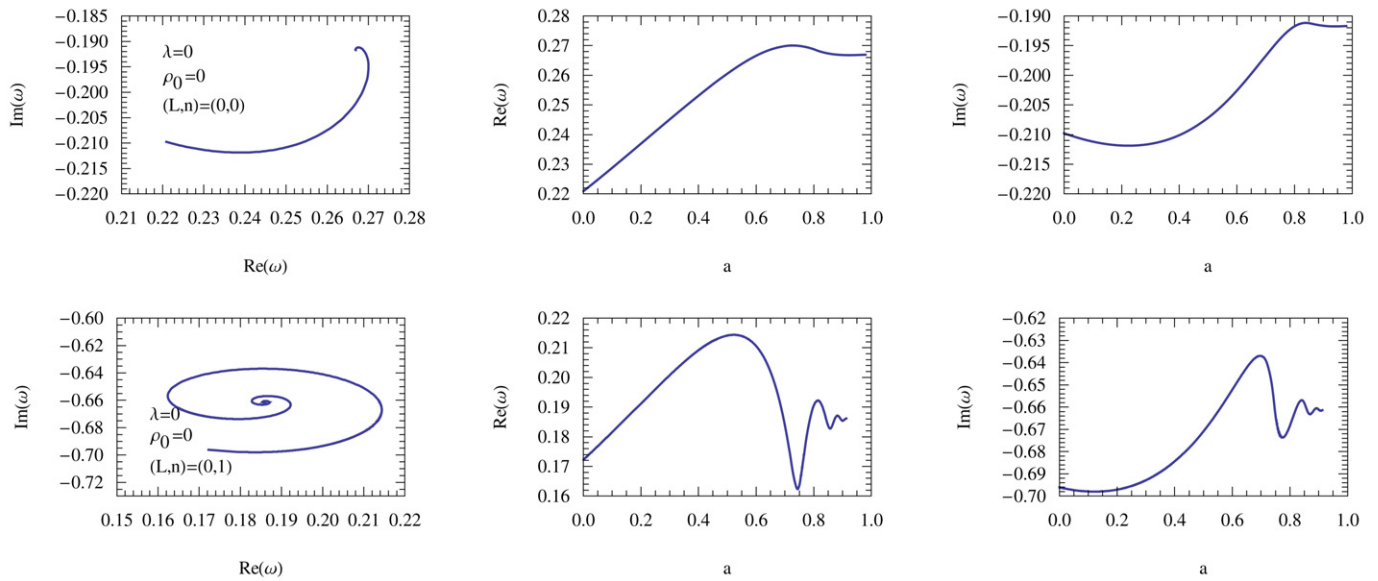


Fig. 1. The left two panels are trajectories in the complex ω plane of scalar QNMs around squashed KK black holes, for $n = 0, n = 1$, with $L = 0$ and $\rho_0 = 0$. The others are real parts ($\text{Re}(\omega)$) and imaginary parts ($\text{Im}(\omega)$) versus parameter $a = 1 - b$.

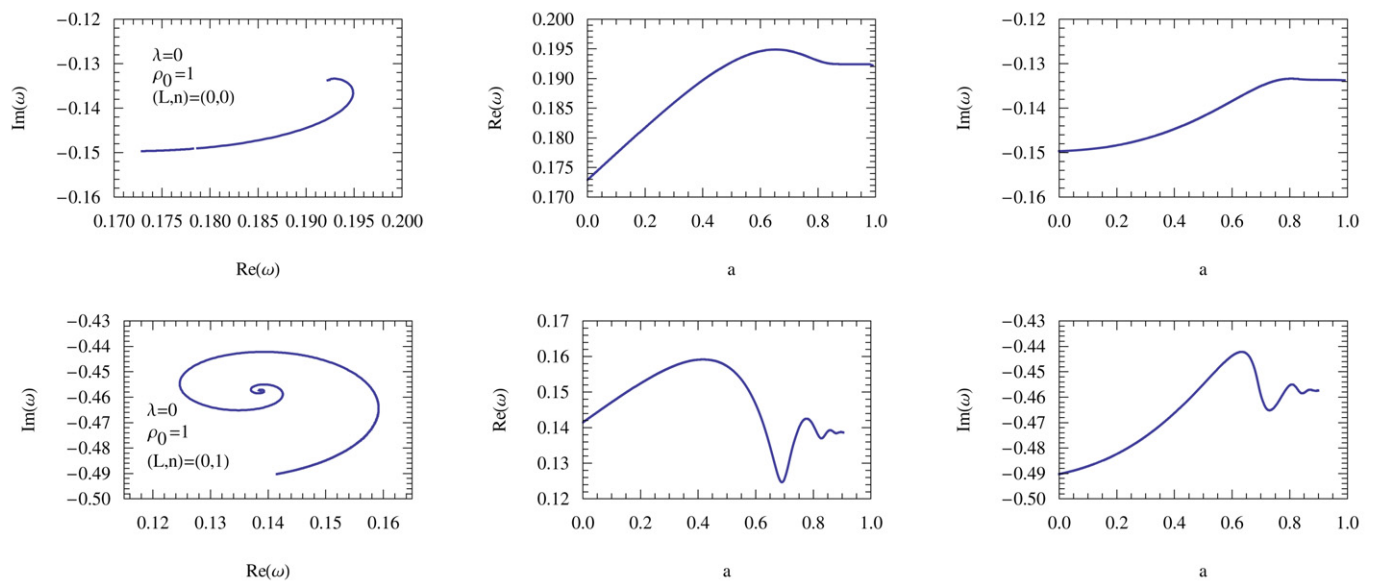


Fig. 2. The left two panels are trajectories in the complex ω plane of scalar QNMs around squashed KK black holes, for $n = 0, n = 1$, with $L = 0$ and $\rho_0 = 1$. The others are real parts ($\text{Re}(\omega)$) and imaginary parts ($\text{Im}(\omega)$) versus parameter $a = 1 - b$.

Table 2

The comparison of values of critical points for QNMs (a_Q) and the singular point of the heat capacity (a_D), when $\lambda = 0$

(λ, L, n, ρ_0)	$\Delta a = a_Q - a_D $	$\frac{\Delta a}{a_Q}$
(0, 0, 1, 0)	0.022	4.21%
(0, 0, 1, 1)	0.016	3.85%
(0, 0, 1, 2)	0.018	3.85%
(0, 1, 4, 0)	0.007	0.953%
(0, 1, 4, 1)	0.0082	2.091%
(0, 1, 4, 2)	0.0041	1.105%

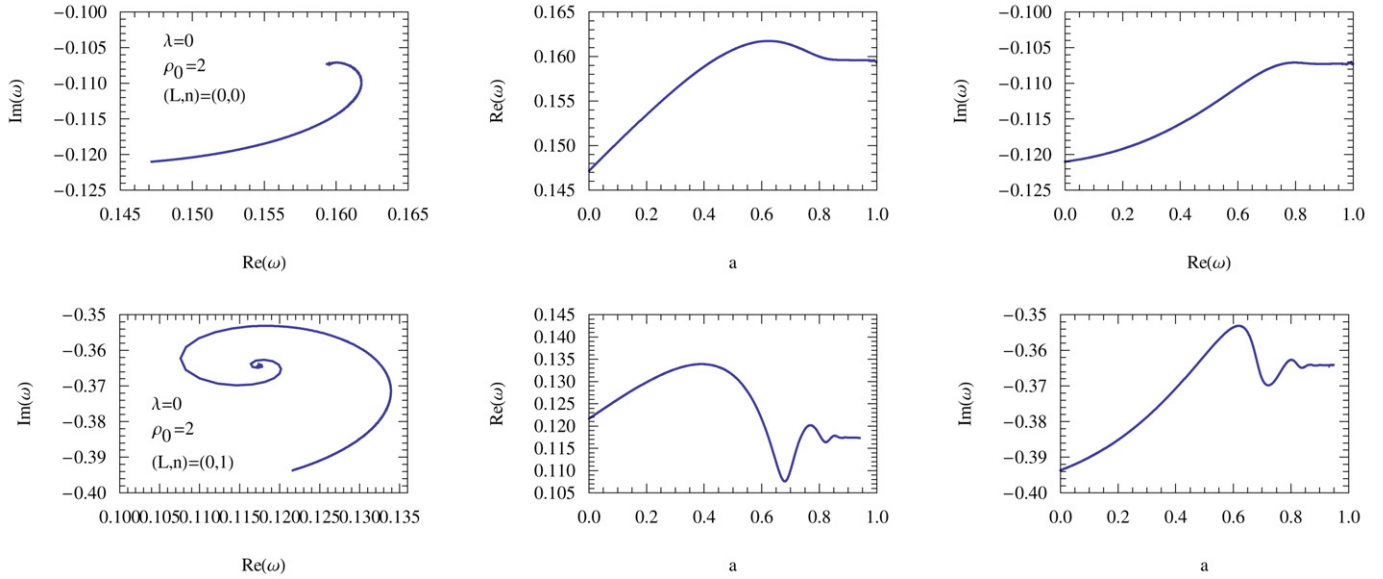


Fig. 3. The left two panels are trajectories in the complex ω plane of scalar QNMs around squashed KK black holes, for $n = 0, n = 1$, with $L = 0$ and $\rho_0 = 2$. The others are real parts ($\text{Re}(\omega)$) and imaginary parts ($\text{Im}(\omega)$) versus parameter $a = 1 - b$.

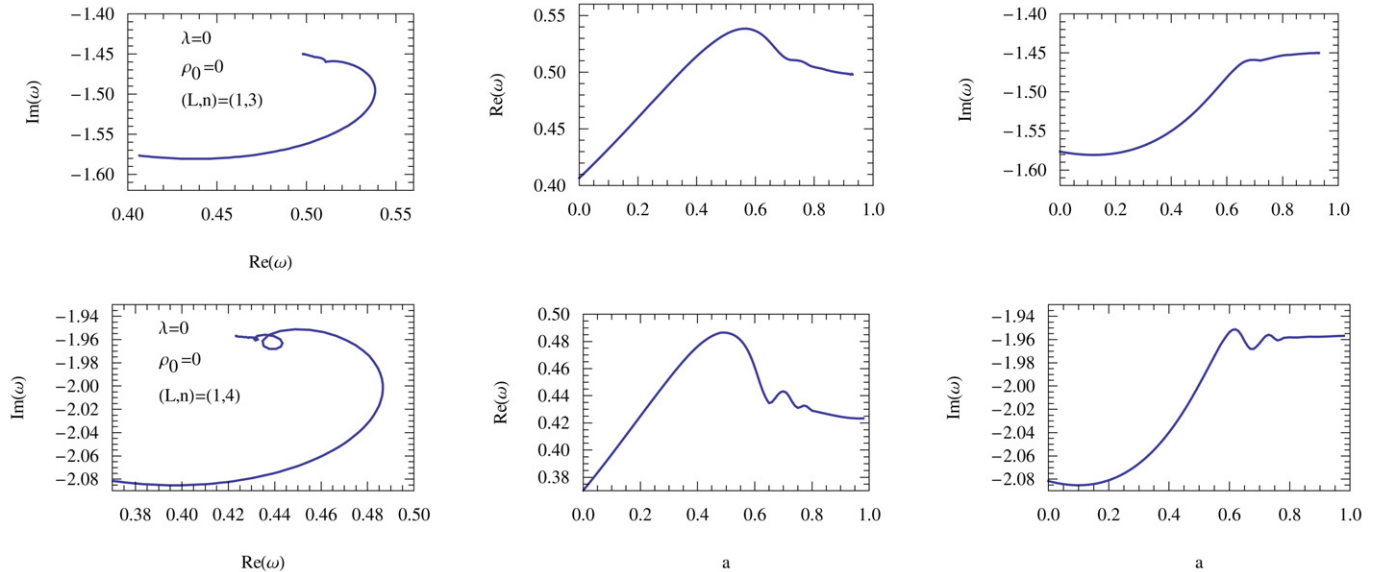


Fig. 4. The left two panels are trajectories in the complex ω plane of scalar QNMs around squashed KK black holes, for $n = 3, n = 4$, with $L = 1$ and $\rho_0 = 0$. The others are real parts ($\text{Re}(\omega)$) and imaginary parts ($\text{Im}(\omega)$) versus parameter $a = 1 - b$.

The heat capacity of the black hole for the fixed Q is given by [25]

$$C_Q = T \left(\frac{\partial S}{\partial T} \right)_Q = \frac{\pi^2 r_+^3 r_\infty^2 - r_-^2}{2} \frac{(r_+^2 - r_-^2)(3r_\infty^4 - r_+^2 r_-^2 - r_\infty^2(r_+^2 + r_-^2))}{r_\infty^2 - r_+^2 r_\infty^4 (5r_-^2 - r_+^2) - r_-^2 (2r_\infty^2 - r_+^2)(3r_+^2 + r_-^2)}. \quad (11)$$

Since $3r_\infty^4 - r_+^2 r_-^2 - r_\infty^2(r_+^2 + r_-^2) > 0$, the sign of the heat capacity C_Q is determined by the term $r_\infty^4(5r_-^2 - r_+^2) - r_-^2(2r_\infty^2 - r_+^2)(3r_+^2 + r_-^2)$ in the denominator. It was found that the Davies' point exists at r_{crit} [25] and one has $C_Q > 0$ for $r_+ < r_{\text{crit}}$ while $C_Q < 0$ for $r_+ > r_{\text{crit}}$

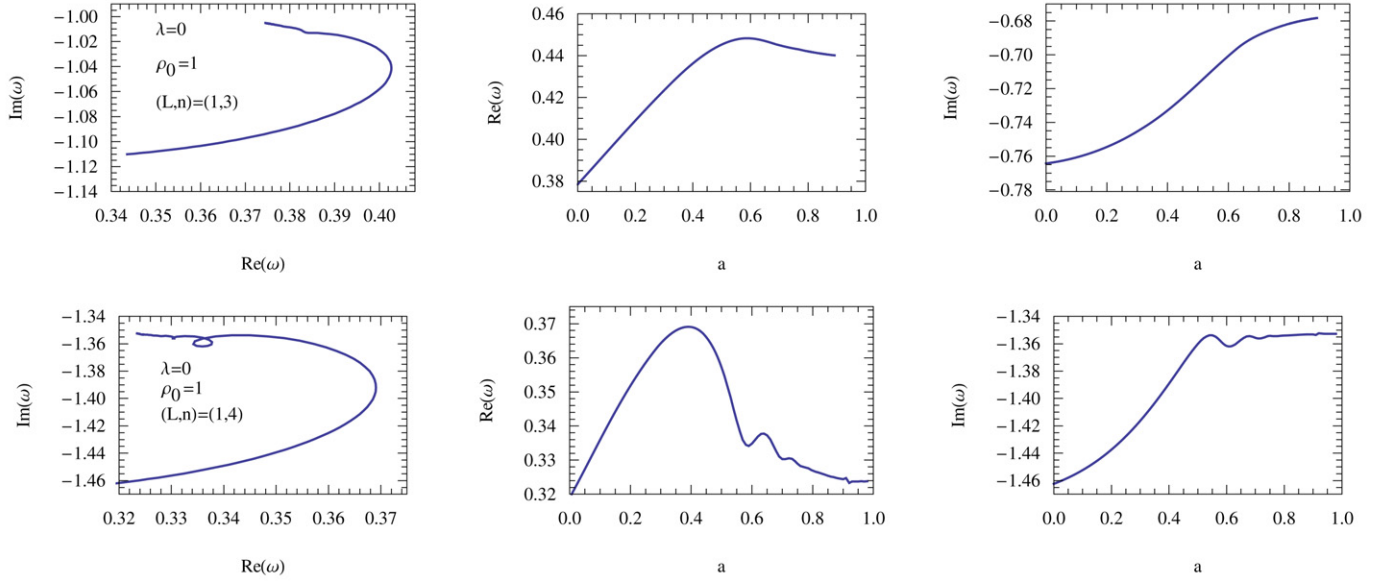


Fig. 5. The left two panels are trajectories in the complex ω plane of scalar QNMs around squashed KK black holes, for $n = 3, n = 4$, with $L = 1$ and $\rho_0 = 1$. The others are real parts ($\text{Re}(\omega)$) and imaginary parts ($\text{Im}(\omega)$) versus parameter $a = 1 - b$.

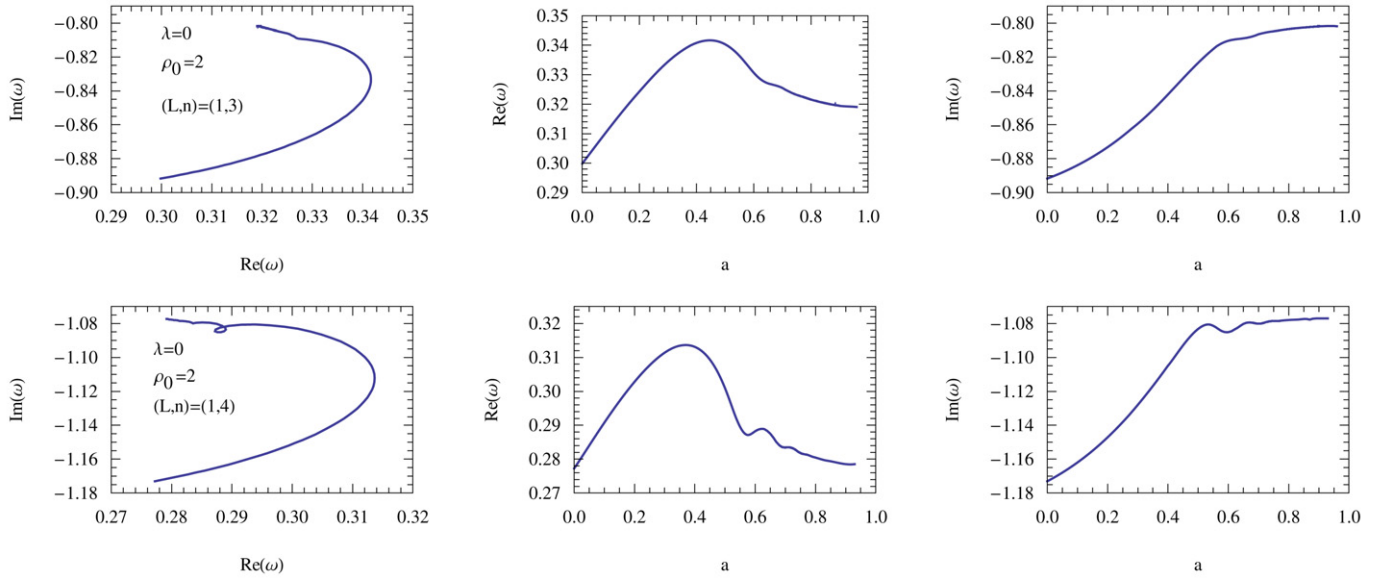


Fig. 6. The left two panels are trajectories in the complex ω plane of scalar QNMs around squashed KK black holes, for $n = 3, n = 4$, with $L = 1$ and $\rho_0 = 2$. The others are real parts ($\text{Re}(\omega)$) and imaginary parts ($\text{Im}(\omega)$) versus parameter $a = 1 - b$.

and C_Q diverges when r_+ crosses this critical value r_{crit} . In the new coordinate, the Davies' point of the divergence of heat capacity C_Q can be obtained from

$$\rho_0(\rho_+ - 5\rho_-) + (\rho_+ - 3\rho_-)(\rho_+ + \rho_-) = 0. \tag{12}$$

If we take $b = \rho_+ - \rho_-$, Eq. (12) can be rewritten as

$$b = \frac{(\rho_+ + \rho_-)(\rho_+ + \rho_- + 2\rho_0)}{2(\rho_+ + \rho_-) + 3\rho_0}. \tag{13}$$

In the limit $\rho_0 \rightarrow 0$, we have $b = (\rho_+ + \rho_-)/2$ and $\rho_+ = 3\rho_-$, which is the Davies' point of thermal stability in the four-dimensional RN black hole. When $\rho_0 \rightarrow \infty$, i.e., $r_\infty \rightarrow \infty$, we obtain $b = 2/3(\rho_+ + \rho_-)$ and $\rho_+ = 5\rho_-$, which is consistent with the Davies' point in five-dimensional RN black hole.

In the following we are going to investigate whether the Davies' points on thermal stability can be reflected in QNM. We will concentrate on the massless scalar perturbation around the charged KK black hole with squashed horizons. The wave equation for the massless scalar field $\Phi(\tau, \rho, \theta, \phi, \psi)$ in the background (6) obeys

$$\frac{1}{\sqrt{-g}} \partial_\mu (\sqrt{-g} g^{\mu\nu} \partial_\nu) \Phi(\tau, \rho, \theta, \phi, \psi) = 0. \tag{14}$$

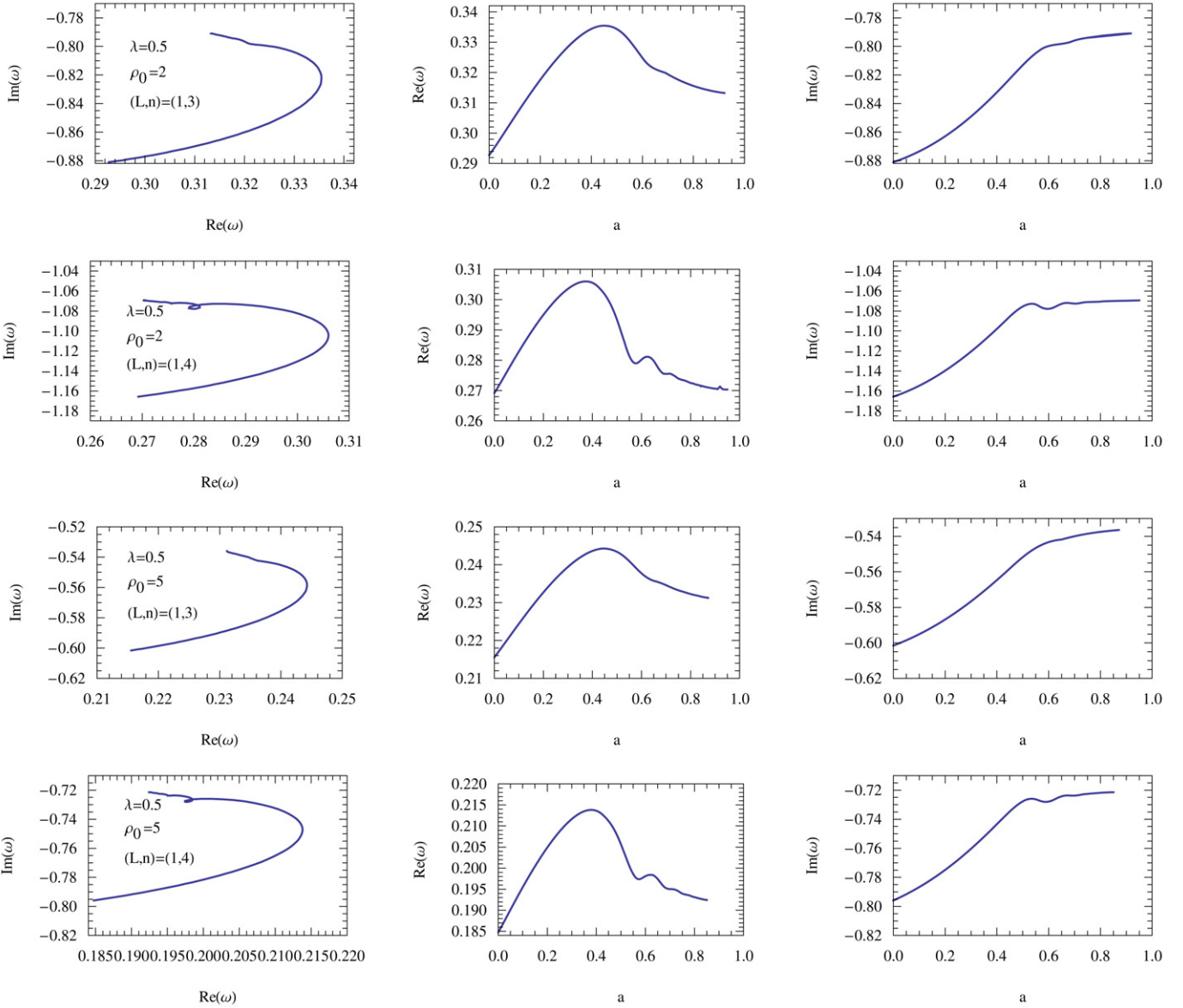


Fig. 7. The left four panels are trajectories in the complex ω plane of scalar QNMs around squashed KK black holes, for $n = 3, n = 4$, with $L = 1, \lambda = 0.5, \rho_0 = 2$ and 5 . The others are real parts ($\text{Re}(\omega)$) and imaginary parts ($\text{Im}(\omega)$) versus parameter a .

Taking the ansatz $\Phi(\tau, \rho, \theta, \phi, \psi) = e^{-i\omega\tau} R(\rho) e^{im\phi + i\lambda\psi} S(\theta)$, where $S(\theta)$ is the so-called spheroidal harmonics, we can obtain the equation

$$\frac{1}{\sin\theta} \frac{d}{d\theta} \left[\sin\theta \frac{d}{d\theta} \right] S(\theta) - \left[\frac{(m - \lambda \cos\theta)^2}{\sin^2\theta} - E_{lm\lambda} \right] S(\theta) = 0, \tag{15}$$

for the angular part. The eigenvalue of this angular equation (15) is $E_{lm\lambda} = L(L + 1) - \lambda^2$. The radial equation reads

$$\frac{F(\rho)}{\rho^2 K^2(\rho)} \frac{d}{d\rho} \left[\rho^2 F(\rho) \frac{dR(\rho)}{d\rho} \right] + [\omega^2 - V(\rho)] R(\rho) = 0, \tag{16}$$

with

$$V(\rho) = F(\rho) \left(\frac{L(L + 1) - \lambda^2}{\rho^2 K^2(\rho)} + \frac{4\lambda^2 K^2(\rho)}{r_\infty^2} \right). \tag{17}$$

The second term in the effective potential came from the fifth dimension of the spacetime. It plays a role of the mass of the field in the radial equation. In general, due to the presence of this term, it is difficult to calculate the QNM through continued fraction method.

Boundary conditions on the wave function $R(\rho)$ at the outer horizon and the spatial infinity can be expressed as

$$R(\rho) \sim \begin{cases} (\rho - \rho_+) \frac{i\rho_+^{3/2} \sqrt{\rho_0 + \rho_+} w}{\rho - \rho_+}, & \rho \rightarrow \rho_+, \\ \rho \frac{i(\rho_0 + 2(\rho_- + \rho_+)) w^2}{2\chi} - \frac{i(2\rho_0 + \rho_- + \rho_+) \lambda^2}{2(\rho_0 + \rho_-)(\rho_0 + \rho_+) \chi} - 1 e^{i\chi\rho}, & \rho \rightarrow \infty. \end{cases} \tag{18}$$

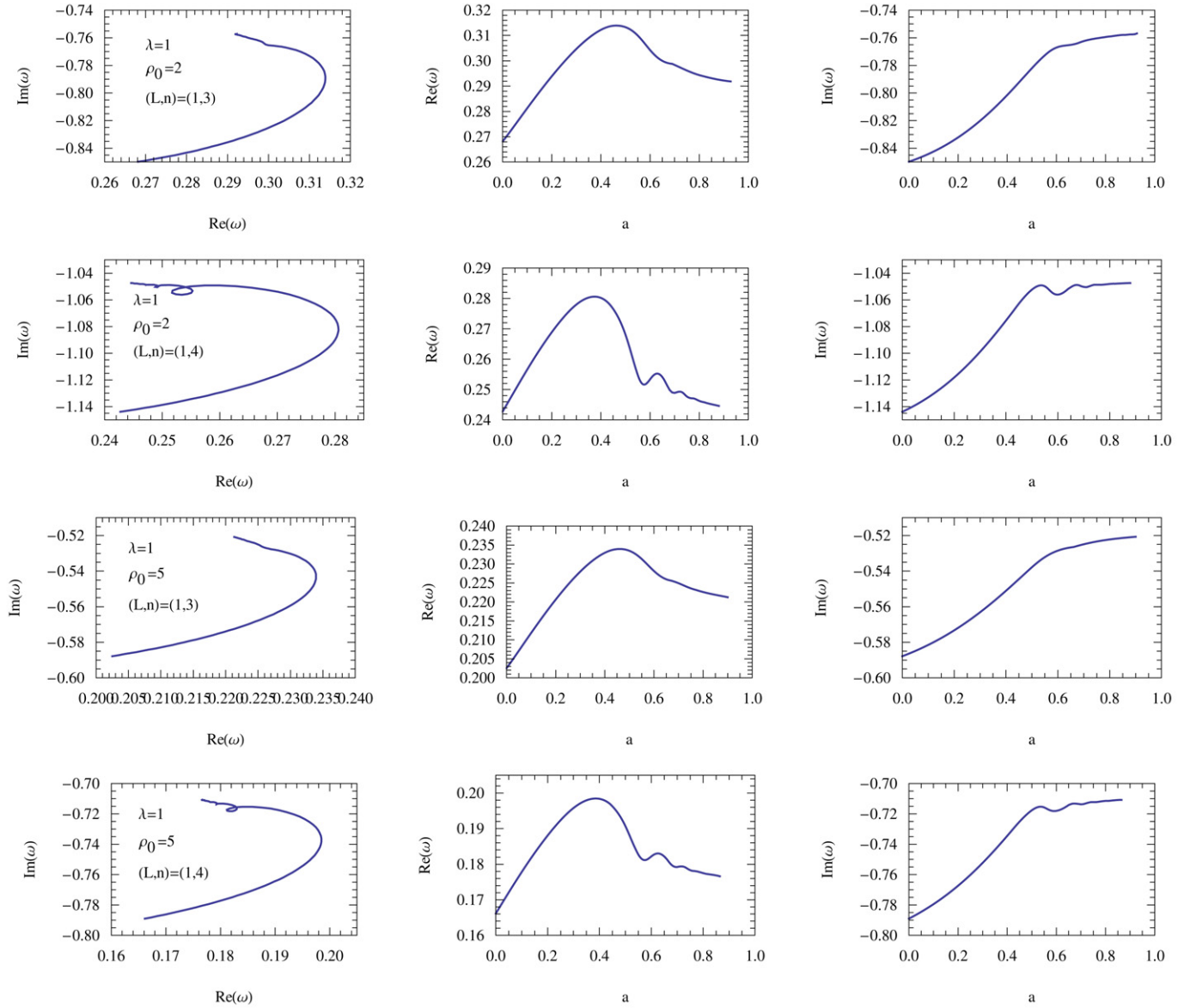


Fig. 8. The left four panels are trajectories in the complex ω plane of scalar QNMs around squashed KK black holes, for $n = 3, n = 4$, with $L = 1, \lambda = 1, \rho_0 = 2$ and 5. The others are real parts ($\text{Re}(\omega)$) and imaginary parts ($\text{Im}(\omega)$) versus parameter a .

Table 3
The comparison of values of critical points for QNMs (a_Q) and the singular point of the heat capacity (a_D), when $\lambda = 0.5$ and $\lambda = 1$

(λ, L, n, ρ_0)	$\Delta a = a_Q - a_D $	$\frac{\Delta a}{a_Q}$
(0.5, 1, 4, 2)	0.0035	0.942%
(0.5, 1, 4, 5)	0.0237	6.29%
(1, 1, 4, 2)	0.0001	0.027%
(1, 1, 4, 5)	0.0330	8.56%

A solution of Eq. (16) that satisfies the above boundary condition can be written as

$$R(\rho) = e^{i(\rho - \rho_-)\chi} (\rho - \rho_-)^{\frac{i\rho_+^{3/2}\sqrt{\rho_0 + \rho_-}\omega}{\rho_+ - \rho_-} + \frac{i[\rho_0 + 2(\rho_- + \rho_+)\omega^2]}{2\chi}} - \frac{i(2\rho_0 + \rho_- + \rho_+)\lambda^2}{2(\rho_0 + \rho_-)(\rho_0 + \rho_+)\chi} (\rho - \rho_+)^{\frac{i\rho_+^{3/2}\sqrt{\rho_0 + \rho_+}\omega}{\rho_- - \rho_+}} \sum_{m=0}^{\infty} a_m \left(\frac{\rho - \rho_+}{\rho - \rho_-}\right)^m, \quad (19)$$

where $\chi^2 = \omega^2 - \frac{\lambda^2}{(\rho_0 + \rho_-)(\rho_0 + \rho_+)}$. The sequence of expansion coefficient $a_m: m = 1, 2, 3, \dots$ is determined by the recurrence relation starting from $a_0 = 1$

$$\alpha_0 a_1 + \beta_0 a_0 = 0, \quad \alpha_m a_{m+1} + \beta_m a_m + \gamma_m a_{m-1} = 0, \quad m = 1, 2, \dots \quad (20)$$

The recurrence coefficients $\alpha_m, \beta_m, \gamma_m$ are given by

$$\alpha_m = m^2 + (C_0 + 1)m + C_0, \quad \beta_m = -2m^2 + (C_1 + 2)m + C_3, \quad \gamma_m = m^2 + (C_2 - 3)m + C_4 - C_2 + 2, \quad (21)$$

where C_m are

$$C_0 = \frac{2i\sqrt{\rho_0 + \rho_+}\omega\rho_+^{3/2}}{\rho_- - \rho_+} + 1, \tag{22}$$

$$C_1 = -\frac{4i\sqrt{\rho_0 + \rho_+}\omega\rho_+^{3/2}}{\rho_- - \rho_+} + \frac{i[(\rho_0 + \rho_-)(\rho_0^2 + 5\rho_+\rho_0 + 4\rho_+^2)\omega^2 + (-2\rho_0 + \rho_- - 3\rho_+)\lambda^2]}{(\rho_0 + \rho_-)(\rho_0 + \rho_+)\chi} - 4, \tag{23}$$

$$C_2 = 3 - \frac{i[\rho_0 + 2(\rho_- + \rho_+)]\omega^2}{\chi} + \frac{2i\rho_+^{3/2}\sqrt{\rho_0 + \rho_+}\omega}{\rho_- - \rho_+} + \frac{i(2\rho_0 + \rho_- + \rho_+)\lambda^2}{(\rho_0 + \rho_-)(\rho_0 + \rho_+)\chi}, \tag{24}$$

$$C_3 = \frac{1}{2(\rho_0 + \rho_-)(\rho_- - \rho_+)(\rho_0 + \rho_+)\chi} \{ \lambda^2 [2(\rho_0 + \rho_+)\chi(\rho_- - \rho_+)^2 + i(-2\rho_0 + \rho_- - 3\rho_+)(\rho_- - \rho_+) + 2\rho_+^{3/2}\sqrt{\rho_0 + \rho_+}(2\rho_0 - \rho_- + 3\rho_+)\omega] - (\rho_0 + \rho_-)(\rho_0 + \rho_+) [(2\rho_+^2(3\rho_0 + 4\rho_+)\chi - i(\rho_- - \rho_+)(\rho_0 + 4\rho_+)\omega^2) + 2\rho_+^{3/2}\sqrt{\rho_0 + \rho_+}((\rho_0 + 4\rho_+)\omega^2 + 2i\chi)\omega + 2(L^2 + L + 1)(\rho_- - \rho_+)\chi] \}, \tag{25}$$

$$C_4 = \frac{(\rho_0 + \rho_-)\omega^2\rho_+^3}{(\rho_+ - \rho_-)^2} + \frac{1}{4} \left\{ \frac{2i\rho_+^{3/2}\sqrt{\rho_0 + \rho_+}\omega}{\rho_- - \rho_+} - \frac{i[\rho_0 + 2(\rho_- + \rho_+)]\omega^2}{\chi} + \frac{i(2\rho_0 + \rho_- + \rho_+)\lambda^2}{(\rho_0 + \rho_-)(\rho_0 + \rho_+)\chi} + 2 \right\}^2. \tag{26}$$

If the boundary condition (18) is satisfied and the series in (20) converge for the given L , the frequency ω is a root of the continued fraction equation

$$\left[\beta_m - \frac{\alpha_{m-1}\gamma_m}{\beta_{m-1}} \frac{\alpha_{m-2}\gamma_{m-1}}{\beta_{m-2}} \dots \frac{\alpha_0\gamma_0}{\beta_0} \right] = \left[\frac{\alpha_m\gamma_{m+1}}{\beta_{m+1}} \frac{\alpha_{m+1}\gamma_{m+2}}{\beta_{m+2}} \frac{\alpha_{m+2}\gamma_{m+3}}{\beta_{m+3}} \dots \right] \quad (m = 1, 2, \dots). \tag{27}$$

This means that we can calculate the QNM frequencies of the charged KK black hole with squashed horizons by solving the above continued fraction equation (27). This equation is impossible to be solved analytically. We can only rely on the numerical calculation to obtain the QNM frequencies.

Taking the limit $Q \rightarrow 0$, we have compared our numerical results by using Leaver’s method with that obtained in [27] by other methods. The comparison is shown in Table 1, which shows good agreement and in addition we see that Leaver’s method we adopted gives more precise result.

In Figs. 1–3 we display the QNM frequencies of scalar perturbation around the squashed KK black holes with charge for $L = 0$, $\lambda = 0$, with overtone numbers $n = 0, 1$ and $\rho_0 = 0, 1, 2$, respectively. We plot both the real part and the imaginary part of QNM frequencies in functions of $a = 1 - b$. Black hole horizons are related to a by $\rho_+ = 1 - a/2$, $\rho_- = a/2$. We observe that over the critical overtone number ($n_c = 1$ for $L = 0$ in the scalar perturbation), both the real part and the imaginary part of QNM frequencies will behave oscillatory when a crosses a critical value a_Q and meanwhile the complex ω plan will exhibit the spiral-like shape. For $\rho_0 = 0$, which is the limiting case of the four-dimensional RN black hole with a twisted S^1 bundle, we observed that the real part of the QNM frequency arrives at its first maximum of its oscillation approximately at the same position as the Davies’ point $a_D = 1/2$. The difference between the critical point from the QNM a_Q from that of the Davies’ point is very small, $|a_Q - a_D| = 0.022$. For ρ_0 not equaling to zero, the Davies’ thermal stability point a_D can be calculated through (12) and from the behavior of QNM frequencies we can read the critical value a_Q when the oscillation of the real and imaginary parts of frequencies start. The results are shown in Table 2. It is interesting to find that critical points got from QNM agree very well to those of Davies’ points.

In Figs. 4–6, we show results for $L = 1$ and $\lambda = 0$, with overtone numbers $n = 3, 4$ and $\rho_0 = 0, 1, 2$, respectively. The Davies’ points are the same for each selected values of ρ_0 no matter the change of L, n . As was observed in [17], with the increase of L , we will observe the spiral-like shape of the complex ω plan and oscillatory real and imaginary frequencies of QNM over higher critical overtone number n_c , namely $n_c = 4$ when $L = 1$ for scalar perturbation. The oscillations of the QNM frequencies start when a over the critical value a_Q , which is again very much in agreement with Davies’ critical point a_D . The results of their differences are shown in Table 2. Choosing very big value of ρ_0 , we observed that the critical point of a from QNM will go towards $1/3$ which is the Davies point for the five-dimensional RN black hole for $\rho_0 \rightarrow \infty$.

In the following we report our results for taking $\lambda \neq 0$. Numerical calculation for the case $\lambda \neq 0$ is much more time consuming than the case with $\lambda = 0$. In Fig. 7, we show results for $L = 1$, $n = 3, 4$ with $\rho_0 = 2, 5$, respectively by choosing $\lambda = 0.5$. In Fig. 8 we show results for the same choice of L, n but with $\lambda = 1$. From these figures, it is obvious that the spiral-like shape still appears at the critical overtone number n_c , namely $n_c = 4$ for $L = 1$ with different ρ_0 and nonzero λ in the scalar perturbation. The critical moment to exhibit the spiral behavior in QNM again agrees well with the Davies thermodynamical point which is shown in Table 3.

In summary we have studied the QNM of scalar perturbation in the background of the charged KK black hole with squashed horizons. We observed that over some critical value of the black hole parameter, both the real part and the imaginary part of the QNMs will experience oscillations and the complex ω plan will exhibit the spiral-like shape. Interestingly this critical value agrees well to the Davies’ point on the thermal stability of black holes obtained from the singular position of the heat capacity. Our limiting case returns to the RN black hole, where the relation was observed in [17]. The correspondence of the critical point observed in QNM to the position of infinite discontinuities of the heat capacities indicates that QNM may shed the light on the turning point of the thermal stability. It is of interest to generalize this discussion to other backgrounds and for different fields’ perturbations.

For a black brane solution it was conjectured that black holes which lack local thermodynamical stability often also lack stability against small perturbations [23]. This conjecture might only hold for black holes with translation symmetry, such as black string. In our background spacetime we observed that on both sides of the turning point of the thermodynamical stability, the imaginary frequencies of the QNM are negative, which tells us that the scalar perturbation is always stable even at the critical point. Recently the metric perturbations were discussed [26,27] and it was indicated that dynamically the squashed KK black hole is stable, this is consistent with our result. This result shows that in the background we are studying it has dynamical stability even when thermodynamical instability

appears. This is quite interesting, which suggests that the relation between the dynamical and thermodynamical stabilities of black holes is non-trivial and further investigations are called for.

Acknowledgements

We thanks J.L. Jing and Q.Y. Pan for helpful discussions. This work was partially supported by NNSF of China, Shanghai Education Commission and Shanghai Science and Technology Commission. S.B. Chen's work was partially supported by the China Postdoctoral Science Foundation under Grant No. 20070410685, the Scientific Research Fund of Hunan Provincial Education Department Grant No. 07B043 and the National Basic Research Program of China under Grant No. 2003CB716300. B. Wang would like to acknowledge the associate programme in ICTP where the work was completed.

References

- [1] H.P. Nollert, *Class. Quantum Grav.* 16 (1999) R159.
- [2] K.D. Kokkotas, B.G. Schmidt, *Living Rev. Rel.* 2 (1999) 2.
- [3] B. Wang, *Braz. J. Phys.* 35 (2005) 1029.
- [4] G.T. Horowitz, V.E. Hubeny, *Phys. Rev. D* 62 (2000) 024027.
- [5] B. Wang, C.Y. Lin, E. Abdalla, *Phys. Lett. B* 481 (2000) 79;
B. Wang, C. Molina, E. Abdalla, *Phys. Rev. D* 63 (2001) 084001;
J.M. Zhu, B. Wang, E. Abdalla, *Phys. Rev. D* 63 (2001) 124004.
- [6] V. Cardoso, J.P.S. Lemos, *Phys. Rev. D* 63 (2001) 124015;
V. Cardoso, J.P.S. Lemos, *Phys. Rev. D* 64 (2001) 084017;
E. Berti, K.D. Kokkotas, *Phys. Rev. D* 67 (2003) 064020;
V. Cardoso, J.P.S. Lemos, *Class. Quantum Grav.* 18 (2001) 5257;
E. Winstanley, *Phys. Rev. D* 64 (2001) 104010;
J. Crisostomo, S. Lepe, J. Saavedra, *Class. Quantum Grav.* 21 (2004) 2801;
S. Lepe, F. Mendez, J. Saavedra, L. Vergara, *Class. Quantum Grav.* 20 (2003) 2417.
- [7] D. Birmingham, I. Sachs, S.N. Solodukhin, *Phys. Rev. Lett.* 88 (2002) 151301;
D. Birmingham, *Phys. Rev. D* 64 (2001) 064024.
- [8] B. Wang, E. Abdalla, R.B. Mann, *Phys. Rev. D* 65 (2002) 084006;
J.S.F. Chan, R.B. Mann, *Phys. Rev. D* 59 (1999) 064025.
- [9] S. Musiri, G. Siopsis, *Phys. Lett. B* 576 (2003) 309;
R. Aros, C. Martinez, R. Troncoso, J. Zanelli, *Phys. Rev. D* 67 (2003) 044014;
A. Nunez, A.O. Starinets, *Phys. Rev. D* 67 (2003) 124013.
- [10] E. Abdalla, B. Wang, A. Lima-Santos, W.G. Qiu, *Phys. Lett. B* 538 (2002) 435;
E. Abdalla, K.H. Castello-Branco, A. Lima-Santos, *Phys. Rev. D* 66 (2002) 104018.
- [11] S. Hod, *Phys. Rev. Lett.* 81 (1998) 4293;
A. Corichi, *Phys. Rev. D* 67 (2003) 087502;
L. Motl, [gr-qc/0212096](#);
L. Motl, A. Neitzke, [hep-th/0301173](#);
A. Maassen van den Brink, [gr-qc/0303095](#);
J. Baez, [gr-qc/0303027](#);
O. Dreyer, *Phys. Rev. Lett.* 90 (2003) 08130;
G. Kunstatter, *Phys. Rev. Lett.* 90 (2003) 161301;
N. Andersson, C.J. Howls, [gr-qc/0307020](#);
V. Cardoso, J. Natario, R. Schiappa, [hep-th/0403132](#).
- [12] V. Cardoso, J.P.S. Lemos, *Phys. Rev. D* 67 (2003) 084020;
K.H.C. Castello-Branco, E. Abdalla, [gr-qc/0309090](#).
- [13] B. Wang, C.Y. Lin, C. Molina, *Phys. Rev. D* 70 (2004) 064025.
- [14] G. Koutsoumbas, S. Musiri, E. Papantonopoulos, G. Siopsis, *JHEP* 0610 (2006) 006;
G. Koutsoumbas, E. Papantonopoulos, G. Siopsis, [arXiv: 0801.4921](#).
- [15] J. Shen, B. Wang, C.Y. Lin, R.G. Cai, R.K. Su, *JHEP* 0707 (2007) 037;
X.P. Rao, B. Wang, G.H. Yang, *Phys. Lett. B* 649 (2007) 472.
- [16] Y.S. Myung, [arXiv: 0801.2434](#).
- [17] J. Jing, Q. Pan, *Phys. Lett. B* 660 (2008) 13.
- [18] P.C.W. Davies, *Proc. R. Soc. London A* 353 (1977) 499;
P.C.W. Davies, *Class. Quantum Grav.* 6 (1989) 1909.
- [19] E. Berti, V. Cardoso, [arXiv: 0802.1889](#).
- [20] D. Pavon, J.M. Rube, *Phys. Rev. D* 37 (1988) 2052;
D. Pavon, *Phys. Rev. D* 43 (1991) 2495;
R.G. Cai, R.K. Su, P.K.N. Yu, *Phys. Rev. D* 48 (1993) 3473;
R.G. Cai, R.K. Su, P.K.N. Yu, *Phys. Rev. D* 52 (1995) 6186;
B. Wang, J.M. Zhu, *Mod. Phys. Lett. A* 10 (1995) 1269.
- [21] O. Kaburaki, I. Okamoto, J. Katz, *Phys. Rev. D* 47 (1993) 2234;
J. Katz, I. Okamoto, O. Kaburaki, *Class. Quantum Grav.* 10 (1993) 1323.
- [22] T. Harmark, V. Niarchos, N.A. Obers, *Class. Quantum Grav.* 24 (2007) R1.
- [23] S.S. Gubser, I. Mitra, [hep-th/0009126](#);
S.S. Gubser, I. Mitra, *JHEP* 0108 (2001) 018;
H.S. Reall, *Phys. Rev. D* 64 (2001) 044005.
- [24] H. Ishihara, K. Matsuno, [hep-th/0510094](#).
- [25] R.G. Cai, L.M. Cao, N. Ohta, *Phys. Lett. B* 639 (2006) 354.
- [26] M. Kimura, K. Murata, H. Ishihara, J. Soda, [arXiv: 0712.4202](#).
- [27] H. Ishihara, M. Kimura, R.A. Konoplya, K. Murata, J. Soda, [arXiv: 0802.0655 \[nucl-th\]](#).